

# Cyclic-N<sub>3</sub>. I. An accurate potential energy surface for the ground doublet electronic state up to the energy of the <sup>2</sup>A<sub>2</sub>/<sup>2</sup>B<sub>1</sub> conical intersection

Dmitri Babikov

Chemistry Department, Marquette University, Wehr Chemistry Building, Milwaukee, Wisconsin 53201-1881

Peng Zhang and Keiji Morokuma

Department of Chemistry, Emory University, Chemistry Building, Atlanta, Georgia 30322

(Received 4 May 2004; accepted 16 June 2004)

A sophisticated adiabatic ground electronic state potential energy surface for a pure nitrogen ring (cyclic-N<sub>3</sub>) molecule is constructed based on extensive high-level *ab initio* calculations and accurate three-dimensional spline representation. Most of the important features of the potential energy surface are presented using various reduced dimensionality slices in internal hyperspherical coordinates as well as full dimensional isoenergy surfaces. Very significant geometric phase effects are predicted in the spectra of rotational-vibrational states of cyclic-N<sub>3</sub>. © 2004 American Institute of Physics. [DOI: 10.1063/1.1780158]

## I. INTRODUCTION

Photodissociation spectra of  $\text{ClN}_3 \rightarrow \text{Cl} + \text{N}_3$  were recorded and the kinetic energy distribution of the  $\text{N}_3$  fragments was derived very recently using a velocity map imaging technique, which also provides a medium-resolution spectra of the internal energy in the  $\text{N}_3$  molecules produced.<sup>1–4</sup> The distribution exhibits a very pronounced bimodal structure and clearly indicates that, in addition to the already known weakly bound linear- $\text{N}_3$  isomer, there exists another energetic form of the  $\text{N}_3$  molecule, with energy about 1.35 eV above the energy of the linear- $\text{N}_3$  isomer. This finding is in very good agreement with recent *ab initio* calculations for  $\text{N}_3$ ,<sup>5</sup> which predicted the existence of a stable ring- $\text{N}_3$  isomer (having the form of an isosceles triangle, called cyclic- $\text{N}_3$  hereafter) at an energy of 1.30 eV above the energy of the linear- $\text{N}_3$  isomer. Cyclic- $\text{N}_3$  is metastable with respect to dissociation to ground state  $\text{N}(^4\text{S}) + \text{N}_2$  ( $\Delta E = -1.4$  eV), which is spin forbidden. Furthermore, very recent unpublished results show that the doublet-quartet surface crossings that must be traversed for dissociation lie about 1 eV above the cyclic- $\text{N}_3$  minimum.<sup>6</sup> Thus, cyclic- $\text{N}_3$  is very stable and carries a lot of energy; it is an excellent new candidate for technological applications in energy storage, high nitrogen explosives, and clean propellants. It is worth mentioning that the nitrogen resources on our planet are practically limitless.

The subject of cyclic- $\text{N}_3$  is still in its infancy. What we know about it was learned from private communications, recent conference presentations, preprints,<sup>6</sup> and a few experimental papers that have recently appeared.<sup>1–4</sup> It is, probably, true to say that experimental studies are somewhat ahead of theory and valuable theoretical guidance in designing experiments and in interpreting experimental results is notably lacking. This paper is the first one in a series of theoretical papers we intend to publish with focus on cyclic- $\text{N}_3$ . In this first paper we present accurate potential energy surface (PES) for cyclic- $\text{N}_3$ . In the second paper in this series<sup>7</sup> we

plan to present calculations of rotational-vibrational states of cyclic- $\text{N}_3$  with particular emphasis on associated geometric phase effects.

Cyclic- $\text{N}_3$  is a Jahn–Teller molecule that exhibits a conical intersection between two of its potential energy surfaces at the  $D_{3h}$  (equilateral triangle) configuration.<sup>6</sup> This conical intersection causes the equilibrium geometry to distort off the  $D_{3h}$  geometry. A further complication is that at the point of conical intersection the symmetry of the Born–Oppenheimer electronic wave function changes. At high enough energies the three-dimensional (3D) vibrational wave function encircles the conical intersection and the standard quantum symmetry selection rules are inappropriate. The geometric phase (known also as Berry's phase) effects should be important in this case and standard theoretical methods for calculations of vibrational states are expected to fail miserably for cyclic- $\text{N}_3$ .

It is difficult to find in the literature a molecule analogous to the cyclic- $\text{N}_3$ . Ozone molecule ( $\text{O}_3$ ) is somewhat similar in a sense that existence of the stable cyclic- $\text{O}_3$  isomer ( $2^1A_2$ ) was very recently predicted theoretically.<sup>8</sup> Cyclic ozone is also an energetic molecule, formed at about 1.3 eV above the energy of usual “open” ozone molecule. However, cyclic ozone is simpler because it has no conical intersection in  $D_{3h}$ , so that no geometric phase effects are expected in the vibrational spectra of cyclic- $\text{O}_3$  and its equilibrium geometry is just an equilateral triangle. Another neighbor of nitrogen in a periodic table, carbon, is also found in an energetic cyclic- $\text{C}_3$  form ( $^3A_2$ ) at 0.85 eV above the energy of its linear “chain” isomer.<sup>9</sup> But again, cyclic- $\text{C}_3$  has no conical intersection in  $D_{3h}$ , its equilibrium structure is an equilateral triangle and its vibrational spectrum must be simpler.

It is quite interesting that in terms of the  $D_{3h}$  conical intersection one can find more similarity between the cyclic- $\text{N}_3$  and several alkali metal trimers. Thus, the  $\text{Na}_3(\text{X})$  has a conical intersection in  $D_{3h}$  and significant geometric phase

effects were theoretically predicted for its vibrational spectra.<sup>10–12</sup> We expect that the cyclic- $N_3$  will be even better example of the geometric phase effects: due to specific features of its potential energy surface, which we describe in this paper, its zero point energy is relatively large and the geometric phase should affect even its ground vibrational state. There are other metal trimers that exhibit a conical intersection in  $D_{3h}$  configuration, e.g.,  $Li_3$  (Refs. 13–16) and  $Cu_3$ .<sup>17–19</sup> However, in both these cases the minimum energy point of the conical intersection descends to very low energies (502 and 555  $cm^{-1}$  above the bottom of the well for  $Li_3(X)$  and  $Cu_3(X)$ , respectively), so that the validity of adiabatic approximation is questionable for the vibrational states at energies well above the pseudorotation barrier. For such vibrational states one has to accomplish nonadiabatic calculations using at least two potential energy surfaces (degenerate at the point of the conical intersection) and including the nonadiabatic coupling between them. This, by itself, is a very complex theoretical and computational problem because of singularities of the nonadiabatic coupling matrix elements at the point of the conical intersection. Furthermore, in such cases it is hard to quantify the importance of the geometric phase effects because they mix with nonadiabatic effects. Alternatively, in the cyclic- $N_3$  the conical intersection is at about 4600  $cm^{-1}$  above the bottom of the well, which should provide us with rare example of a “clean” geometric phase effect.

In Sec. II of the paper we briefly describe *ab initio* methods used for calculations of cyclic- $N_3$  energies. Section III gives details about the hyperspherical coordinates used to set up a 3D grid and describes construction of a 3D spline of the PES between the *ab initio* points. In Sec. IV we describe all the important features of the PES. Discussion of possible geometric phase effects is given in the Conclusions.

## II. AB INITIO METHOD

The nature of the electronic wave function around the cyclic- $N_3$  minimum is very complicated. Recent *ab initio* calculations<sup>6</sup> indicated that there are two stationary points around this region,  $^2A_2$  and  $^2B_1$  in terms of the symmetry of wave functions. However, these two  $C_{2v}$  structures have different  $C_2$  axes and  $\sigma_v$  planes, and they originate from the Jahn-Teller distortion of the degenerate  $^2E''$  components. In addition, the *ab initio* calculations showed that  $^2A_2$  structure is the transition state connecting two equivalent  $^2B_1$  local minima with a very small barrier.

The accurate description of N–N bonds requires a large atomic basis set. In the present work, Dunning’s standard correlation consistent polarized valence triple-zeta basis set augmented with diffuse functions (aug-cc-pVTZ) was employed. As we are focusing our attention on the study of bound states near the cyclic- $N_3$  minimum region, we are mainly interested in calculations of the ground electronic state.

Regarding the multiconfiguration nature of the cyclic- $N_3$  radical, internally contracted multireference configuration interaction with all singles and doubles (MRCISD) wave functions<sup>20</sup> was used to construct the adiabatic potential energy surface. To all MRCISD energies we applied the multi-

reference version of the Davidson correction<sup>21</sup> that can be denoted as MRCISD(Q). In the MRCISD(Q) calculations, the reference wave function was obtained from the corresponding full valence CASSCF calculations consisting of 15 electrons distributed in 12 molecular orbitals, and only the 1s orbitals of N atoms were kept doubly occupied in all configurations while the remaining 15 electrons were correlated, denoted as MRCISD(Q) (15e/12o) aug-cc-pVTZ. The MOLPRO 2002.6 program was used to perform all the calculations.<sup>22</sup>

## III. COORDINATE SYSTEM AND 3D SPLINE

In this work we describe the positions of nitrogen nuclei in the cyclic- $N_3$  triatomic molecule using adiabatically adjusting principal-axes hyperspherical (APH) coordinates.<sup>23,24</sup> In terms of the usual mass scaled internal Jacobi coordinates  $(r, R, \alpha)$ , the APH coordinates  $(\rho, \theta, \phi)$  are defined as follows:

$$\rho = \sqrt{R^2 + r^2}, \quad \rho \in [0, \infty]; \quad (1)$$

$$\tan \theta = \frac{\sqrt{(R^2 - r^2)^2 + (2Rr \cos \alpha)^2}}{2Rr \sin \alpha}, \quad \theta \in [0, \pi/2]; \quad (2)$$

$$\tan \phi = \frac{2Rr \cos \alpha}{R^2 - r^2}, \quad \phi \in [0, 2\pi]. \quad (3)$$

Qualitatively, the value of the hyperradius  $\rho$  is a measure of the overall “size” of a triatomic molecule. Hyperangles  $\theta$  and  $\phi$  describe changes in its “shape.”

Often used with APH coordinates is the stereographic projection,<sup>23</sup> which is a convenient way to plot a 2D slice of the PES at a fixed value of the hyperradius  $\rho$ , while  $\theta$  and  $\phi$  are allowed to vary. This corresponds to variation of the “shape” of the triatomic molecule keeping its overall “size” constant. In such a 2D plot the energy is a function of two Cartesian variables  $x$  and  $y$  defined as

$$x = \cos \phi \tan(\theta/2), \quad (4)$$

$$y = \sin \phi \tan(\theta/2), \quad (5)$$

where  $-1 \leq x \leq 1$ ,  $-1 \leq y \leq 1$ . With such a choice the center of the plot ( $x=0, y=0$ ) corresponds to  $\theta=0$  and describes the triatomic molecule in  $D_{3h}$  geometry (equilateral triangle). The distance of any point from the center of the plot is determined by the  $\theta$  variable only,

$$\sqrt{x^2 + y^2} = \tan(\theta/2). \quad (6)$$

Points at the unit circle  $x^2 + y^2 = 1$  correspond to  $\theta = \theta_{\max} = \pi/2$  and describe linear configurations of the  $N_3$  triatomic system (not studied in this paper). Stereographic projections will be used many times throughout the following section.

Using APH coordinates we have set up a dense  $(\rho, \theta, \phi)$  grid in three dimensions:  $\rho(\text{a.u.}) = \{3.19; 3.209; 3.236; 3.264; 3.294; 3.324; 3.37; 3.42; 3.4656; 3.51; 3.555; 3.6; 3.648; 3.697; 3.754; 3.812; 3.872; 3.93\}$ ,  $\tan(\theta/2) = \{0; 0.01; 0.023; 0.0396; 0.0557; 0.069; 0.081; 0.0942; 0.1079; 0.1202; 0.134; 0.144; 0.1534; 0.1642; 0.1753; 0.19; 0.21; 0.23; 0.25\}$ , and  $\phi = \{0; 10^\circ; 20^\circ; 30^\circ; 40^\circ; 50^\circ; 60^\circ\}$ . Our grid contains only seven equidistant points in  $\phi$  because the PES is

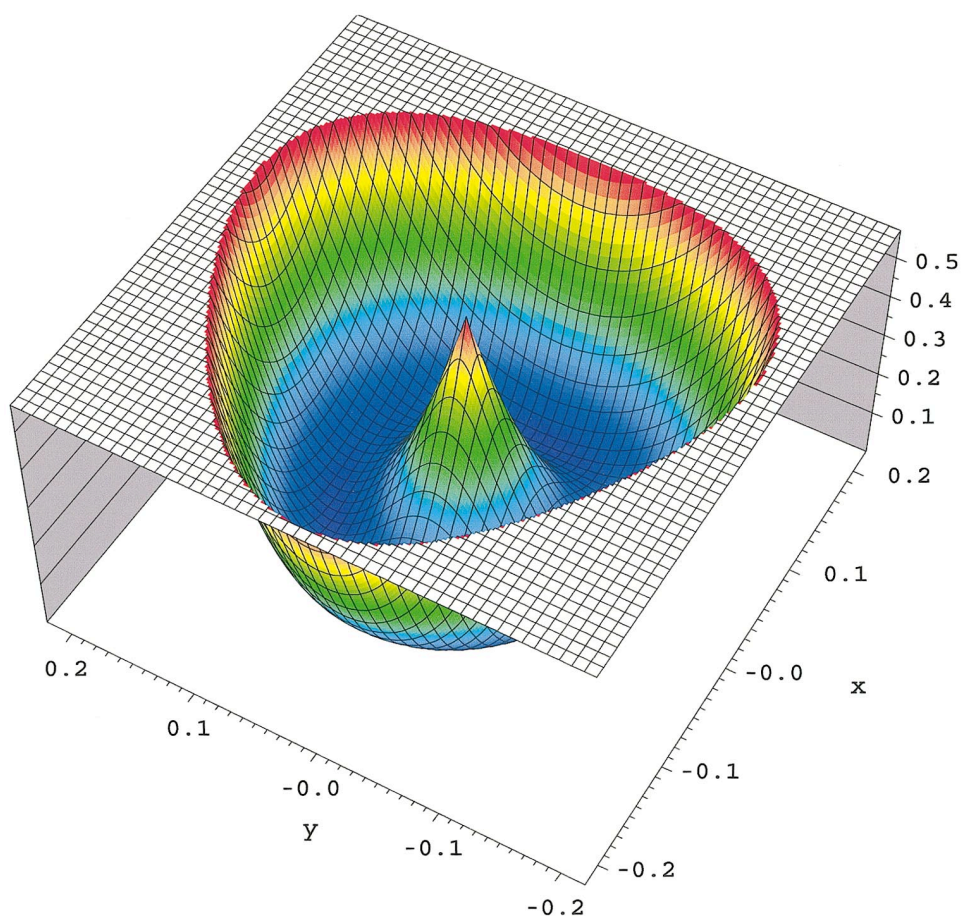


FIG. 1. (Color) A surface plot for stereographic projection of the cyclic-N<sub>3</sub> PES. The value of the hyperradius is fixed at  $\rho=3.4070$  a.u. The conical intersection is seen at  $(x=0, y=0)$ . The vertical scale shows the energy in eV.

quite smooth along this coordinate, i.e., the energy does not change rapidly as the observer goes around the conical intersection. This will be clearly demonstrated in the next section and is one of the advantages offered by the APH coordinates. Along the  $\rho$  and  $\theta$  coordinates the energy of cyclic-N<sub>3</sub> changes significantly and we had to develop a much denser nonregular grid for these two coordinates. First, we performed calculations on a sparser initial grid and then, when the general topology of the surface was already known, we added additional grid points for accuracy of surface representation. Such a procedure resulted in a total of 2286 points determined *ab initio*. Among them, 18 points ( $\theta=0$ ) are in  $D_{3h}$ ,  $18 \times 18 \times 2 = 648$  points ( $\phi=0$  and  $60^\circ$ ) are in  $C_{2v}$ , and  $18 \times 18 \times 5 = 1620$  points are in  $C_s$  symmetry.

Finally, an accurate three-dimensional interpolant has been constructed between the *ab initio* points using the tensor product  $B$ -cubic spline representation.<sup>25</sup> The resulting PES thoroughly covers the energy range up to the conical intersection. In this part of configuration space, covered by an interpolant on a 3D grid, the surface representation is very accurate. In addition, we have constructed a 1D extrapolant along  $\theta$  coordinate onto the region outside of the grid, i.e., behind the value of  $\tan(\theta/2) = 0.25$ , using a simple quadratic function. The PES is not accurate in that region, but such a smooth extension will be necessary for future dynamics calculations of the vibrational states. Extrapolation in  $\phi$  coordinate is unnecessary; due to periodicity all physical values of  $\phi$  are covered by the grid.<sup>23</sup> Extrapolation in hyperradius  $\rho$  is

not required either, because the relevant range of  $\rho$ , to be scanned by the sector-adiabatic approach,<sup>24</sup> is thoroughly covered by the grid.

#### IV. MAJOR FEATURES OF THE PES

Although APH hyperspherical coordinates are very useful and are not new,<sup>23</sup> they are not yet widely employed for analysis and representation of the potential energy surfaces of triatomic molecules. To introduce readers to this subject we first show several simpler 2D and 1D slices through the hypersphere of the PES for cyclic-N<sub>3</sub>.

Crossing of the potential energy surfaces for  ${}^2A_2$  and  ${}^2B_1$  electronic states in cyclic-N<sub>3</sub> forms a seam along the  $D_{3h}$  symmetry line and is, generally, a curve (1D) in the three-dimensional space. Energy of the crossing point is a smooth function of the size of equilateral triangle; it exhibits a minimum and this minimum energy point is further called the minimum point of conical intersection. Previous calculations<sup>6</sup> have identified the geometry of the  ${}^2A_2/{}^2B_1$  minimum conical intersection as an equilateral triatomic with a bond length of 1.3699 Å.

In the APH coordinates the crossing seam is just along the  $\rho$  axis ( $\theta=0, \phi=0$ ) and the minimum point of conical intersection is at  $\rho = 3.4070$  a.u. Figure 1 shows a 2D slice of the PES when  $\rho$  is kept constant at this value while  $\theta$  and  $\phi$  are varied. The conical intersection is clearly seen at  $\theta=0$  and is surrounded by a deep attractive well. The energy of

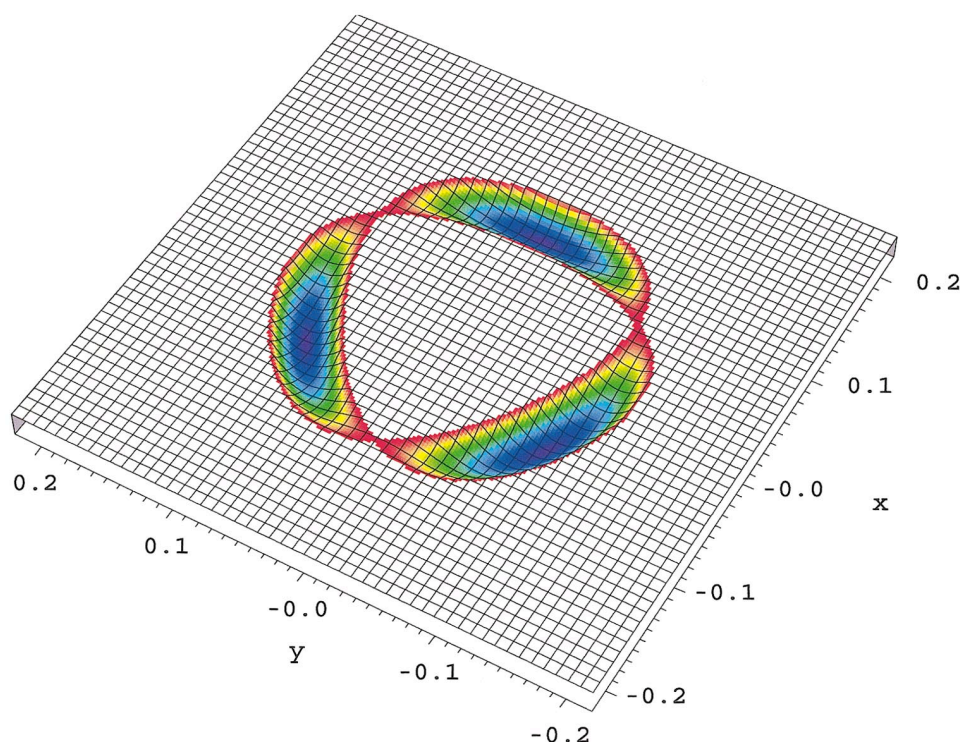


FIG. 2. (Color) A surface plot for stereographic projection of the cyclic- $N_3$  PES. The value of the hyperradius is fixed at  $\rho=3.4656$  a.u. The low energy part of surface is shown from zero to  $\sim 0.0386$  eV. Three shallow minima, separated by three transition states, are clearly seen.

the conical intersection is 0.57 eV above the cyclic- $N_3$  minimum, which is taken as the energy reference point throughout this and future papers. The geometry of the minimum was previously identified<sup>6</sup> as an isosceles triangle ( $C_{2v}$ ) with an apex angle of  $49.86^\circ$  and two equal sides of  $1.4659 \text{ \AA}$ . On a global surface there are three such equilibrium minima; they correspond to the three possible permutations of N nuclei within cyclic- $N_3$ . In the APH coordinates the three minima are at  $\rho=3.4656$  a.u.,  $\tan(\theta/2)=0.1079$ , and  $\phi=\{0;120^\circ;240^\circ\}$ . They are clearly seen in Fig. 2, where a 2D-slice of the PES is shown with  $\rho$  fixed at 3.4656 a.u. while  $\theta$  and  $\phi$  are varied. The three minima are separated by three low energy transition states at 0.0386 eV. Their signatures are also clearly seen in Fig. 2 at  $\phi=\{60^\circ;180^\circ;300^\circ\}$ . At the point of a transition state the cyclic- $N_3$  is an isosceles triangle ( $C_{2v}$ ) with an apex angle of  $71.93^\circ$  and two equal sides of  $1.3058 \text{ \AA}$ ,<sup>6</sup> which corresponds to  $\rho=3.4469$  a.u. and  $\tan(\theta/2)=0.1138$  in the APH coordinates. Here it is worth mentioning that the shape of the cyclic- $N_3$  at the minimum energy point is an acute triangle; at the transition state point it is an obtuse triangle. This correspondence reverses for all metal trimers mentioned in the introduction section ( $Li_3$ ,  $Na_3$ , and  $Cu_3$ ).<sup>12,16,18</sup>

Figure 3(a) shows a 1D slice of the surface presented in Fig. 2 by a vertical plane, which passes through the three critical points: a point of conical intersection, a minimum point at  $\phi=0$ , and a transition state point at  $\phi=180^\circ$ . The energy scale in Fig. 3(a) is chosen to show the PES up to the conical intersection, not seen at the energy scale of Fig. 2. Figure 3(a) demonstrates a crossing of two electronic states of different symmetry at the point of a conical intersection. On the left side of the intersection, where the transition state is located, the electronic state symmetry is  $^2A_2$ , while on the right side of the conical intersection, where the minimum is

located, the electronic state symmetry is  $^2B_1$ . Another convenience of APH coordinates is important in this context. In the APH coordinates all geometries of this triatomic molecule with  $\phi=n\pi/3$  ( $n$  is integer) belong to  $C_{2v}$  point group. Those cyclic- $N_3$  geometries that exhibit  $^2B_1$  symmetry of the ground electronic state, including three minimum points, correspond to  $\phi=\{0;120^\circ;240^\circ\}$ , while all  $N_3$  geometries with  $^2A_2$  symmetry of the ground electronic state, including three transition state points, correspond to  $\phi=\{60^\circ;180^\circ;300^\circ\}$ . This property, valid for all values of  $\rho$  and  $\theta$ , is depicted in Fig. 3(b), where the surface of Fig. 2 is presented as a 2D contour plot, superimposed with  $C_{2v}$  symmetry map. All three minima and all three transition states are now shown and the symmetry of the electronic state along constant  $\phi=n\pi/3$  directions is given for each case,  $n=\{0,1,2,3,4,5\}$ . This useful property was employed to select electronic states of correct symmetry during *ab initio* calculations. A “shape legend” is given at the bottom of Fig. 3(b) in order to simplify understanding of the hyperspherical coordinates and to show how the shape of cyclic- $N_3$  triatomic molecule changes as the observer goes from the minimum point ( $\circ$ ) to the transition state point ( $\bullet$ ), either through the point of conical intersection ( $*$ ) following the  $C_{2v}$  symmetry line, or following the minimum energy path (along  $\phi$  coordinate). It is also very useful to remember that a displacement along the hyperradius  $\rho$  corresponds to symmetric stretch of the cyclic- $N_3$  triatomic molecule, while displacements along the hyperangles  $\theta$  and  $\phi$  correspond to the bend and asymmetric stretch, respectively.

Finally, we have scanned the PES of cyclic- $N_3$  and have determined, for each value of the hyperradius  $\rho$ , the energies of the three critical points: the conical intersection, the minimum, and the transition state point. These data are collected in Fig. 4(a). All three curves are smooth and the three

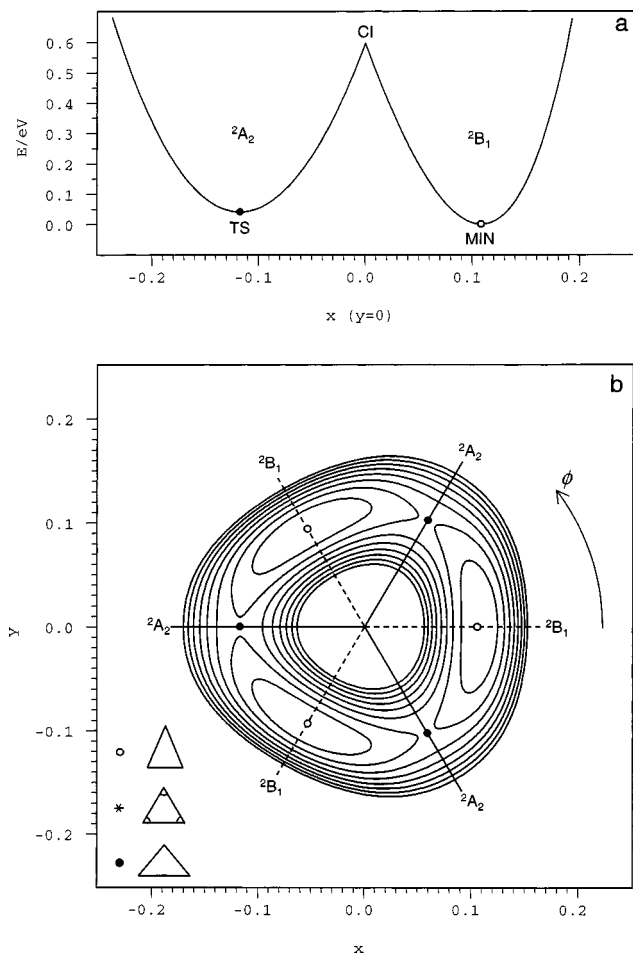


FIG. 3. Electronic state symmetries of the cyclic-N<sub>3</sub> PES: (a) A slice of Fig. 2 by a vertical plane which passes through the  $y=0$  line. TS is a transition state point and MIN is a minimum; CI is a point of conical intersection. The electronic state symmetry of the adiabatic ground state PES changes at the point of CI; (b) A contour map of Fig. 2. Contour lines are given from 0 to 0.16 eV in steps of 0.02 eV. Three solid and three dashed lines cross at the point of CI and indicate  ${}^2A_2$  and  ${}^2B_1$  electronic state symmetries, respectively. See the text for discussion. In both frames the symbol  $\circ$  indicates points of minima and the symbol  $\bullet$  indicates transition state points. A “shape legend” is given at the bottom of Fig. 3(b). The scales of stereographic coordinate  $x$  are the same in both frames.

minima at  $\rho=3.4070$ ,  $3.4469$ , and  $3.4656$  a.u. (see discussion above) are clearly seen. Vertical dotted lines are drawn through the minima. For the minimum energy points and the transition state points we have also determined their values of the hyperangle  $\theta$ , i.e., their distances from the point of conical intersection. The second derivatives of energy along  $\theta$  coordinate have also been determined for the minimum energy points and the transition state points. All these data are collected in Fig. 4(b) as a function of the hyperradius  $\rho$ . Figures 4(a) and 4(b) demonstrate that the reference value of the hyperradius  $\rho$ , which accurately represents all features of the PES, can barely be found. Therefore, we conclude that it is impossible to construct an accurate and simple  $E \otimes e$  model<sup>12</sup> of the cyclic-N<sub>3</sub>. Actual data plotted in Fig. 4 are available for download as EPAPS documents<sup>26</sup> and can be used by those readers who want to derive parameters for a crude  $E \otimes e$  model of cyclic-N<sub>3</sub> PES.

Now we present several 3D views of the PES for cyclic-

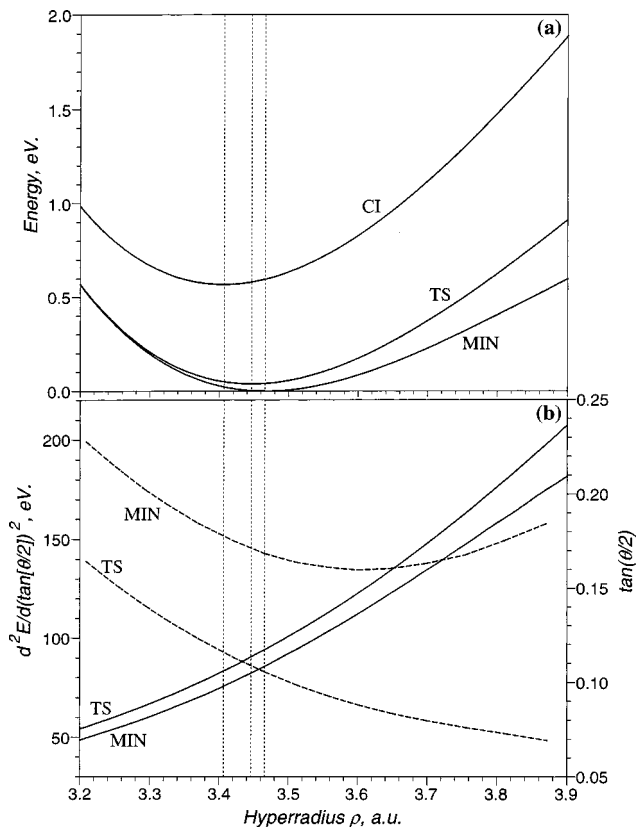


FIG. 4. Scan of the cyclic-N<sub>3</sub> PES: (a) Energies of the three critical points as a function of the hyperradius. Vertical dotted lines are drawn through the three minima; (b) Positions of the MIN and TS points (solid lines, right vertical axis) and the second derivatives of energy at those points (dashed lines, left vertical axis) as a function of the hyperradius.

N<sub>3</sub> using a different approach: All three APH variables ( $\rho$ ,  $\theta$ ,  $\phi$ ) are varied and an isoenergy surface at a fixed value of the energy (constant energy surface) is plotted. This represents a part of 3D configuration space that can be accessed by nitrogen nuclei at a constant value of vibrational energy in the cyclic-N<sub>3</sub> triatomic, i.e., the three-dimensional classically allowed region. The hyperradius  $\rho$  is plotted in the vertical direction [see Fig. 5(a)] and increases from the bottom of the figure to its top. Stereographic projection variables  $x$  and  $y$  [Eqs. (4) and (5)] are plotted in the two horizontal directions. We found this approach the most useful and compact for analysis of global features of the PES. Figure 5 shows two such views of the PES at low energies. Figure 5(a) gives the isoenergy surface at energy of 0.02 eV, i.e., below the transition state. The three cyclic-N<sub>3</sub> minima, discussed earlier in the text, are very well separated at this energy. If the vibrational zero-point energy of cyclic-N<sub>3</sub> would be small enough, so that a vibrational eigenstate could form at this energy (which is not the case, see below), the vibrational wave function for such a state would exhibit three separate blobs and describe three independent 3D oscillators, each sitting in its own well. Figure 5(b) shows the isoenergy surface at the energy of the transition state: 0.0386 eV. This figure shows in all three dimensions how the three transition states separate three cyclic-N<sub>3</sub> minima.

Figure 6 shows two isoenergy surfaces at 0.162 and 0.52 eV. According to our preliminary calculations,<sup>7</sup> the first of

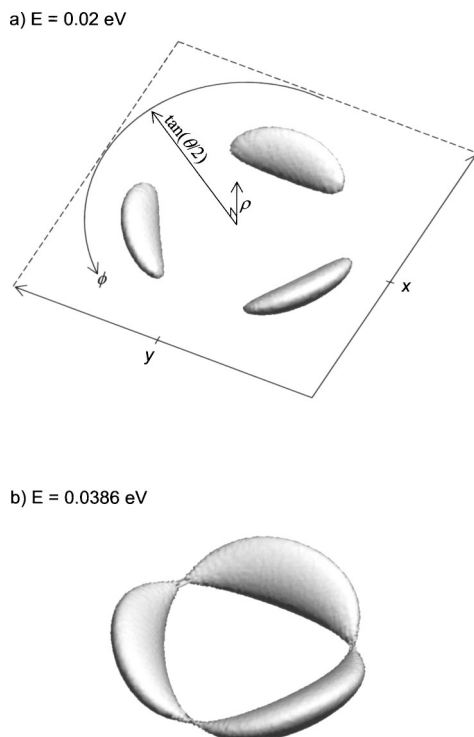


FIG. 5. Isoenergy surfaces of the cyclic- $N_3$  PES: (a) Low value of energy, about midway between the minimum and the transition state energy. Hyper-spherical coordinates ( $\rho$ ,  $\theta$ ,  $\phi$ ) and stereographic projection coordinates ( $x$ ,  $y$ ) are shown for reference; (b) Energy is equal to the energy of the transition state. The isoenergy surface exhibits nodes at the three transition state points.

them is roughly equal to the energy of the ground vibrational state of cyclic- $N_3$  (zero-point vibrational energy); the second energy was chosen just 0.05 eV below the conical intersection. Therefore, energy range between the energies of Figs. 6(a) and 6(b) is the window where the vibrational states of the ground electronic state cyclic- $N_3$  are located. Calculations of the vibrational states for cyclic- $N_3$  in this energy range are ongoing and will be reported elsewhere.<sup>7</sup> The isoenergy surface in Fig. 6(a) exhibits a quite unusual shape; it is basically a torus with the conical intersection at its center, i.e., a torus encircling the conical intersection. All three minima and three transition states are inside of the surface of the torus, quite close to its internal circumference, so that at the energy of Fig. 6(a) one can easily exchange nitrogen nuclei in  $N_3$ -triatomic molecule, which corresponds to moving an observer along the internal circumference of the torus (along  $\phi$  coordinate) around the conical intersection. In a more standard interpretation this corresponds to going from one of the three cyclic- $N_3$  minima to any other one over the corresponding transition state. An isoenergy surface at high energy, shown in the Fig. 6(b), exhibits some specific structure in addition to a toroidal-like behavior. It still surrounds the conical intersection but now the hole inside the torus, where the conical intersection is located, is quite small. (At the energy of the conical intersection the isoenergy surface becomes similar to a *horn* torus, a torus with no hole in the middle.<sup>27</sup>) Closer look at the outside part of the PES shows that six extended parts start developing in the vicinity of the  $C_{2v}$  symmetry planes; at even higher energy three of these

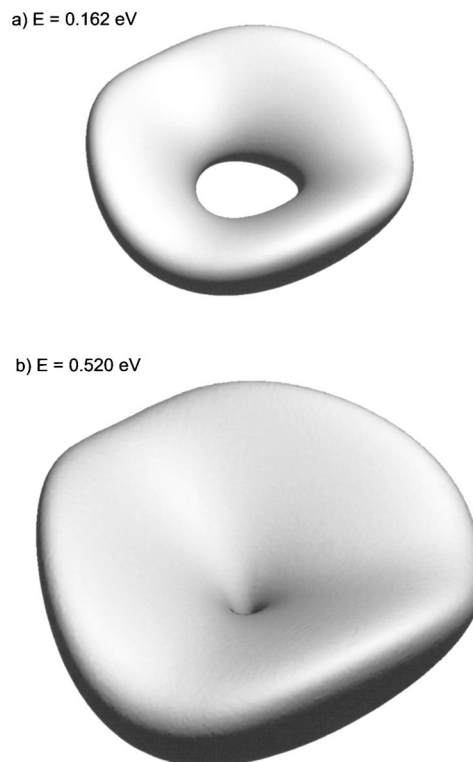


FIG. 6. Isoenergy surfaces of the cyclic- $N_3$  PES: (a) Energy value approximately equal to energy of the ground vibrational state; (b) High value of energy, just below the conical intersection. Isoenergy surfaces exhibit toroidal shape and encircle the conical intersection.

structures around  $\phi = \{0; 120^\circ; 240^\circ\}$  will be transformed into the three dissociation channels, and the other three around  $\phi = \{60^\circ; 180^\circ; 300^\circ\}$  will make the three transition states for isomerization to linear- $N_3$ .<sup>6</sup>

## V. CONCLUSIONS

Analysis of the 3D PES for the cyclic- $N_3$  molecule using isoenergy surfaces in hyperspherical coordinates provides us with good visual understanding of a general topology of the PES and even gives some ideas about the general shape of the vibrational wave functions for cyclic- $N_3$ . Indeed, the vibrational wave function for the ground vibrational state will occupy a toroidal-like part of space around the conical intersection, very similar to that shown in Fig. 6(a). Vibrational wave functions for excited vibrational states will, of course, develop nodes in three dimensions and, as seen from Fig. 6(b), will occupy larger volumes in 3D configuration space, preserving the overall toroidal-like structure. Vibrational frequencies, automatically calculated by standard *ab initio* packages using harmonic approximation and limited information about the PES in the vicinity of the minimum point, are wrong because the wells around the cyclic- $N_3$  minima are too shallow to accommodate any vibrational states. It is interesting that even the ground vibrational state wavefunction covers all three minima and three transition state points simultaneously.

Even in the case of the ground vibrational state the symmetry of electronic wave function changes six times as the vibrational wave function goes around the conical intersec-

tion. Indeed, as seen in Fig. 3(b), the “torus” crosses the  $\phi = \{0; 120^\circ; 240^\circ\}$  planes, where the symmetry is  ${}^2B_1$  and three minima are located, as well as the  $\phi = \{60; 180^\circ; 300^\circ\}$  planes, where the symmetry is  ${}^2A_2$  and three transition state points are located. Therefore, there should be an important effect of the geometric phase on the energies of all the vibrational states in cyclic-N<sub>3</sub>, including the ground vibrational state. This effect should clearly manifest itself in experiments, even through the excitation of cyclic-N<sub>3</sub> fundamental frequencies.

The next important step will be quantum dynamics calculations of the bound rotational-vibrational states of cyclic-N<sub>3</sub> and construction of the corresponding infrared spectra. Such calculations are underway.<sup>7</sup> This information would be very helpful for experimental groups in development of spectroscopic techniques for unambiguous detection, accurate analysis, and characterization of cyclic-N<sub>3</sub>.

### ACKNOWLEDGMENTS

The authors would like to acknowledge Professor Alec Wodtke, University of California at Santa Barbara, for bringing the subject of cyclic-N<sub>3</sub> to the attention of our theoretical groups. The authors thank Brian Kendrick and Russell T Pack in Los Alamos for many helpful conversations and encouragement. The work was in part supported by a grant at Emory University from the Air Force Office of Scientific Research (Grant No. FA9550-04-1-0080). Computer resources were provided by MPP2 computational facilities at EMSL at Pacific Northwest National Laboratory as well as by the Cherry Emerson Center for Scientific Computation at Emory University.

<sup>1</sup>N. Hansen and A. M. Wodtke, *J. Phys. Chem. A* **107**, 10608 (2003).

<sup>2</sup>N. Hansen, A. M. Wodtke, A. V. Komissarov, and M. C. Heaven, *Chem. Phys. Lett.* **368**, 568 (2002).

<sup>3</sup>N. Hansen, A. V. Komissarov, K. Morokuma, M. C. Heaven, and A. M. Wodtke, *J. Chem. Phys.* **118**, 10485 (2003).

<sup>4</sup>D. Matsiev, J. Chen, M. Murphy, and A. M. Wodtke, *J. Chem. Phys.* **118**, 9477 (2003).

<sup>5</sup>M. Bittererova, H. Ostmark, and T. Brink, *J. Chem. Phys.* **116**, 9740 (2002).

<sup>6</sup>P. Zhang, K. Morokuma, N. Hansen, and A. M. Wodtke, *J. Chem. Phys.* (to be published).

<sup>7</sup>D. Babikov, B. K. Kendrick, P. Zhang, and K. Morokuma (unpublished).

<sup>8</sup>R. Siebert and R. Schinke, *J. Chem. Phys.* **119**, 3092 (2003).

<sup>9</sup>A. M. Mebel and R. I. Kaiser, *Chem. Phys. Lett.* **360**, 139 (2002), and references therein.

<sup>10</sup>B. Kendrick, *Phys. Rev. Lett.* **79**, 2431 (1997).

<sup>11</sup>B. Kendrick, *Int. J. Quantum Chem.* **64**, 581 (1997).

<sup>12</sup>B. Kendrick, *J. Phys. Chem. A* **107**, 6739 (2003).

<sup>13</sup>W. H. Gerber and E. Schumacher, *J. Chem. Phys.* **69**, 1692 (1978).

<sup>14</sup>M. Mayer and L. S. Cederbaum, *J. Chem. Phys.* **105**, 4938 (1996).

<sup>15</sup>H.-G. Kramer, M. Keil, C. B. Suarez, W. Demtroder, and W. Meyer, *Chem. Phys. Lett.* **299**, 212 (1999).

<sup>16</sup>M. Keil, H.-G. Kramer, A. Kudell, M. A. Baig, J. Zhu, W. Demtroder, and W. Meyer, *J. Chem. Phys.* **113**, 7414 (2000).

<sup>17</sup>T. C. Thompson, D. G. Truhlar, and C. A. Mead, *J. Chem. Phys.* **82**, 2392 (1985).

<sup>18</sup>C. P. Walch and B. C. Laskowski, *J. Chem. Phys.* **84**, 2734 (1986).

<sup>19</sup>D. G. Truhlar, T. C. Thompson, and C. A. Mead, *Chem. Phys. Lett.* **127**, 287 (1986).

<sup>20</sup>H.-J. Werner and P. J. Knowles, *J. Chem. Phys.* **89**, 5803 (1988).

<sup>21</sup>E. R. Davidson, *J. Comput. Phys.* **17**, 87 (1975).

<sup>22</sup>MOLPRO 2002.1, a package of *ab initio* programs designed by H.-J. Werner and P. J. Knowles, R. D. Amos, A. Bernhardsson, A. Berning *et al.*

<sup>23</sup>R. T Pack and G. A. Parker, *J. Chem. Phys.* **87**, 3888 (1987).

<sup>24</sup>B. K. Kendrick, R. T Pack, and R. B. Walker, *J. Chem. Phys.* **110**, 6673 (1999), and references therein.

<sup>25</sup>Carl de Boor, *A Practical Guide to Splines* (Springer, New York, 1978).

<sup>26</sup>See EPAPS Document No. E-JCPSA6-121-314431 for energies and positions of the three critical points as functions of the hyperradius in cyclic-N<sub>3</sub> (Fig. 4). A direct link to this document may be found in the online article's HTML reference section. The document may also be reached via the EPAPS homepage (<http://www.aip.org/pubservs/epaps.html>) or from [ftp.aip.org](ftp://ftp.aip.org) in the directory /epaps/. See the EPAPS homepage for more information.

<sup>27</sup>See A. Gray, *Modern Differential Geometry of Curves and Surfaces with Mathematica*, 2nd ed. (CRC, Boca Raton, FL, 1997), pp. 304–306 or go at <http://mathworld.wolfram.com/HornTorus.html>